atmosphere

MDPI

Article

A Multiscale Tiered Approach to Quantify Contributions: A Case Study of $PM_{2.5}$ in South Korea During 2010–2017

Minah Bae [1], Byeong-Uk Kim [2], Hyun Cheol Kim [3,4] and Soontae Kim [1,*]

[1] Department of Environmental and Safety Engineering, Ajou University, Suwon 16499, Korea; bma829@ajou.ac.kr

[2] Georgia Environmental Protection Division, Atlanta, GA 30354, USA; byeonguk.kim@gmail.com

[3] Air Resources Laboratory, National Oceanic and Atmospheric Administration, College Park, MD 20740, USA; hyun.kim@noaa.gov

[4] Cooperative Institute for Satellite Earth System Studies, University of Maryland, College Park, MD 20740, USA

* Correspondence: soontaekim@ajou.ac.kr

Received: 17 January 2020; Accepted: 25 January 2020; Published: 27 January 2020

Abstract: We estimated long-term foreign contributions to the particulate matter of 2.5 μm or less in diameter ($PM_{2.5}$) concentrations in South Korea with a set of air quality simulations. The Weather Research and Forecasting (WRF)-Sparse Matrix Operator Kernel Emissions (SMOKE)-Community Multiscale Air Quality (CMAQ) modeling system was used to simulate the base and sensitivity case after a 50% reduction of foreign emissions. The effects of horizontal modeling grid resolutions (27- and 9-km) was also investigated. For this study, we chose $PM_{2.5}$ in South Korea during 2010–2017 for the case study and emissions from China as a representative foreign source. The 9-km simulation results show that the 8-year average contribution of the Chinese emissions in 17 provinces ranged from 40–65%, which is ~4% lower than that from the 27-km simulation for the high-tier government segments (particularly prominent in coastal areas). However, for the same comparison for low-tier government segments (i.e., 250 prefectures), the 9-km simulation presented lowered the foreign contribution by up to 10% compared to that from the 27-km simulation. Based on our study results, we recommend using high-resolution modeling results for regional contribution analyses to develop an air quality action plan as the receptor coverage decreases.

Keywords: $PM_{2.5}$; long-range transport; source-receptor relationship; receptor coverage; model horizontal grid resolution

1. Introduction

Many cities in South Korea often experience high particulate matter of 2.5 μm or less in diameter ($PM_{2.5}$) levels that exceed the $PM_{2.5}$ National Ambient Air Quality Standard [1]. With the rise in public concern about $PM_{2.5}$ concentration, the South Korean government has developed and implemented various emission reduction measures to lower the $PM_{2.5}$ concentration in the country [2,3]. When developing an effective air quality management plan, it is essential to understand key factors affecting the $PM_{2.5}$ concentration, such as the major contributors [4].

Previous studies have attempted to quantify the contributions of foreign and domestic sources to $PM_{2.5}$ concentrations in Northeast Asian countries [5–7]. Itahashi et al. [8] reported that contributions from China, South Korea, and Japan to the ambient sulfate concentration over Oki Island were 46–50%, 5–15%, and approximately 1%, respectively, via a chemical transport model. Uno et al. [7] concluded that contributions to fine-mode nitrate in Japan from Northeast Asian sources

outside of the country can reach 85%. Among the past studies, two specifically examined variability in domestic and foreign contributions for South Korea. Kim et al. [6] estimated that the foreign contribution to particulate matter of 10 μm or less in diameter (PM_{10}) in the Seoul Metropolitan Area (SMA) is approximately 60% of the annual PM_{10} concentration. They also reported that contributions to the annual $PM_{2.5}$ concentrations from domestic and foreign sources can vary by 20% or more depending on the meteorological and emission conditions. Choi et al. [5] reported that the Chinese contribution to South Korean $PM_{2.5}$ concentrations was up to 68% during May and June 2016.While they exhibited one consensus that long-range transport of air pollutants is important to elucidate local air quality over the region, one potential major drawback of these studies is that they employed a single modeling domain with a coarse horizontal grid resolution ranging from 25–80 km while focusing on regional scale air pollution.

Recently, the local governments in South Korea have been tasked with analyzing the cause of their $PM_{2.5}$ problems and to prepare their corresponding air quality improvement plans. This means that they need to account for $PM_{2.5}$ and its precursors due to local emissions with high horizontal resolution as well as the long-range transport of air pollutants. However, the area of a South Korean local prefecture is 382 km^2 on average, which is too small to be evaluated at 25–80 km resolutions. At the same time, South Korea itself has very high population densities in many cities along with highly developed industrial complexes, which has resulted in significant local pollution emission contributions toward its own air quality degradation [9,10]. Therefore, it is necessary to perform air quality simulations with a fine-grid resolution to quantify the impact of local source impacts while a coarse-grid resolution is sufficient to estimate the contributions of the long-range transport of pollutants due to remote upwind sources such as Chinese emissions.

For these reasons, a modeling approach needs to reconcile estimating the long-range transport of $PM_{2.5}$ from Northeast Asian countries along with regional sources to understand the domestic and foreign contributions to the $PM_{2.5}$ levels of specific regions as quantifying both of these contributions is crucial for pollution control policy-making. The focus of our study comprises two goals: (a) to quantify the contribution of foreign emission sources to the $PM_{2.5}$ concentration in South Korea and (b) to explore the associated uncertainties in the selection of the analysis method. For this, we designed a multiscale tiered contribution analysis approach to assess local and regional $PM_{2.5}$ contributions in space and time. Section 2 offers a description of the multiscale modeling configuration and approach used in this study, while Section 3 presents the impact of foreign emissions on local $PM_{2.5}$ concentrations at different government tiers (i.e., province (high-tier) vs. prefecture (low-tier)) in South Korea.

2. Data and Methodology

2.1. Observations

In this study, we used surface temperature and wind speed observations from the Meteorological Aerodrome Reports (METAR) data for the evaluation of the meteorological model simulation; 98 sites in China and South Korea were considered. $PM_{2.5}$ composition ground observation data were provided by the National Institute of Environmental Research. Air quality observations at six supersites in South Korea were used for the long-term model performance evaluation.

2.2. The Modeling Domain and Study Period

Considering the horizontal scale of transboundary transport (100 s of km) of air pollutants in Northeast Asia, a coarse horizontal grid resolution (e.g., 25–80 km) may be sufficient to investigate the foreign source apportionment or impact [5–8]. At the same time, air quality simulation with a fine horizontal grid resolution (e.g., 9- or 3-km) is desirable to examine detailed spatial distributions of local emissions, terrain height, and population so as to better represent the source-receptor relationships [11]. However, air quality simulation with a fine horizontal grid resolution requires

heavy computational resources such as long computing time and large data storage for the input and output data [12].

To overcome the aforementioned limitations and to perform computationally efficient contribution estimation, we used a nested modeling domain in this study (Figure 1): an outer domain with a 27-km horizontal grid resolution to cover major emission regions in Northeast Asia and an inner domain with a 9-km horizontal grid resolution over the Korean Peninsula. For the temporal scale, we note that recent meteorological changes in Northeast Asia had affected air quality in the region [13,14]. Therefore, we attempted to account for the effect of interannual variability of meteorology on the estimated contributions by conducting 8-year-long (2010–2017) simulations in this study. The long-term simulation also gave us the opportunity to acquire more robust seasonal variations of contribution estimation than is possible via a single year simulation.

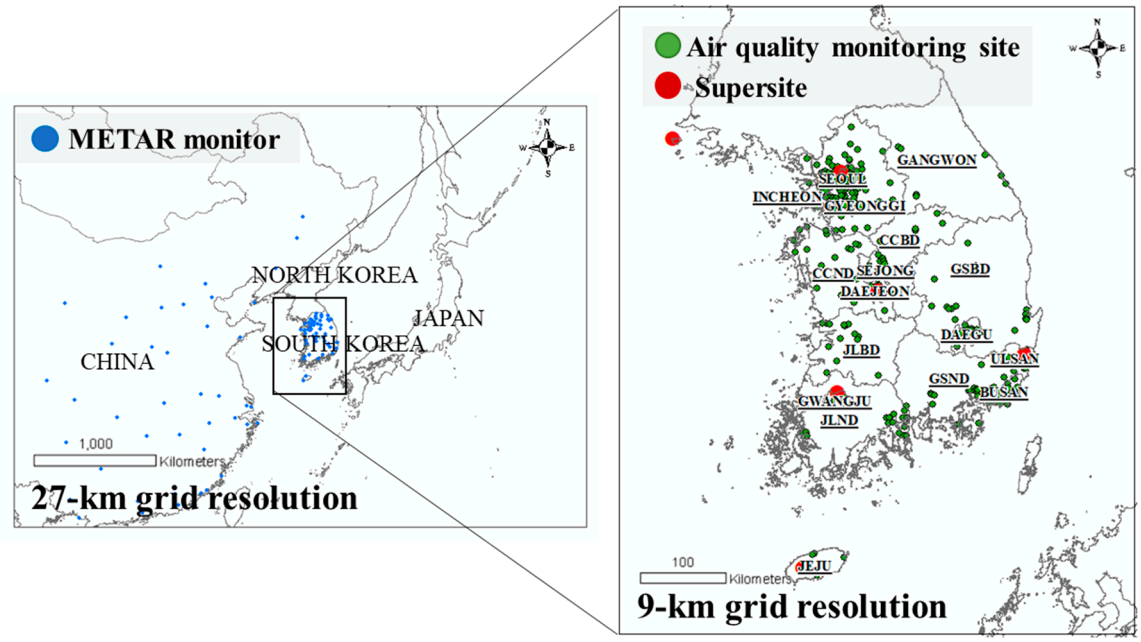

Figure 1. Modeling domains, meteorological stations, and air quality monitoring sites. The 27- and 9-km grid domains have 174 × 128 cells and 67 × 82 cells, respectively. The blue dots represent METeorological Aerodrome Reports (METAR) monitors. The green and red circles depict the urban air quality monitoring sites (AMS) and six supersites, respectively.

2.3. Air Quality Simulation

2.3.1. Model Description

For the air quality simulations, we used the Community Multiscale Air Quality (CMAQ; [15]) model version 4.7.1. It is a 3-dimensional chemical transport model that can be used to estimate regional and local air quality. Meteorological input data were prepared with Weather Research and Forecasting (WRF; [16]) model version 3.4.1. The WRF output data were processed with the Meteorology-Chemistry Interface Processor (MCIP) version 3.6 to prepare model-ready meteorological input files [15]. Biogenic emission input data were developed with the Model of Emission of Gases and Aerosols from Nature (MEGAN) [17]. Anthropogenic emission data were further processed with Sparse Matrix Operator Kernel Emissions (SMOKE; [18]) to prepare model-ready hourly emission input files.

2.3.2. Meteorological and Emission Input Data

The National Centers for Environmental Prediction-Final (NCEP-FNL; [19]) products were used for the WRF meteorological model as the initial and boundary conditions. In the case of Korean anthropogenic emission input data, we used the Clean Air Policy Support System (CAPSS) 2010 [20]

from the National Institute of Environmental Research of Korea. The CAPSS 2010 estimated South Korean anthropogenic emissions for around 1000 source classification codes (SCCs), including energy production, industrial and non-industrial combustion, manufacturing and production processes, energy storage, solvent use, on-road and off-road mobiles, agriculture, waste treatment, and fugitive sources. For foreign anthropogenic emissions, we utilized the Model Inter-Comparison Study for Asia 2010 (MICS-Asia; [21]). MICS-Asia is a mosaic of Asian emission inventories such as REAS2, MEIC, etc. Emissions in the MICS-Asia 2010 are classified into five categories: power, industry, residential, transportation, and agriculture.

For this study, we only used one set of anthropogenic emission inventories but developed biogenic emissions for each modeling year. This setup provides a modeling platform on which we can examine the effects of anthropogenic emission changes in $PM_{2.5}$ concentrations and contributions while accounting for meteorological variation and associated biogenic emission changes.

2.3.3. Model Setup

We used the WSM 6-class for Micro Physics and YSU for the PBL schemes. We used the CMAQ with the Statewide Air Pollution Research Center, Version 99 (SAPRC99) [22], a chemical mechanism for gaseous chemical reactions and AERO5 for aerosol processes. More details of the WRF configurations and the CMAQ configuration are reported in Table 1.

Table 1. The WRF and CMAQ configurations used in the study.

WRF Version 3.4.1		**CMAQ Version 4.7.1**	
Micro Physics	WSM 6-class	Aerosol Module	AERO5
Cumulus Scheme	Kain-Fritsch	Chemical Mechanism	SAPRAC 99
Long-Wave Radiation	RRTM	Advection Scheme	YAMO
Short-Wave Radiation	Goddard	Horizontal Diffusion	Multiscale
PBL Scheme	YSU	Vertical Diffusion	Eddy
		Cloud Scheme	RADM

2.4. The Sensitivity Modeling Approaches

Two sets of these based on the brute force method (BFM) were used to investigate the Chinese contribution to South Korean $PM_{2.5}$ concentrations (Table 2). First, we performed base and sensitivity simulations with a single 27-km horizontal grid domain, as shown in Figure 1. The base simulation included all of the emission sources from China and South Korea. The sensitivity simulation was conducted after a 50% reduction of the Chinese anthropogenic emissions (referred to as the 27-km simulation hereafter).

Second, we used two modeling domains: one at 27-km grid (coarse) resolution and the other at 9-km grid (fine) resolution to estimate foreign and local emission contributions, respectively, to the $PM_{2.5}$ concentration at the prefectural level in the downwind area. We applied a multiscale tiered method to resolve the foreign and local contributions for a small-sized prefecture. The simulations at the 27-km grid resolution provided foreign emission sensitivity for the daughter 9-km grid domain. With the foreign emission sensitivity nested in the mother domain, simulations at the 9-km grid resolution could be used to estimate the foreign and local emission contributions at a finer receptor resolution (referred to as the 9-km simulation hereafter). High-resolution modeling can elaborate spatial distributions of emissions and allow modelers to better account for the characteristics of the emissions [23,24].

Table 2. Details of the two sets of air quality simulations.

Simulation	Horizontal Grid Resolution	Description
Traditional	27-km	- One single domain. - Base and sensitivity runs are conducted with the same modeling domain.
In this study	27- and 9-km	- Two nested modeling domains. - Simulations on the mother model domain (i.e., 27-km) to prepare boundary conditions for the simulations on the daughter model domain (i.e., 9-km) for both the base and sensitivity runs. - Simulations on the daughter model domain to estimate the foreign contribution on a finer model grid.

We estimated the absolute Chinese contribution by calculating the zero-out contribution (ZOC):

$$ZOC = (C_{base} - C_{\Delta E}) \times \frac{100\%}{\Delta E} \quad (1)$$

and the relative Chinese contribution by

$$Contribution\ (\%) = \frac{ZOC}{C_{base}} \times 100\%, \quad (2)$$

where C_{base} and $C_{\Delta E}$ represent the concentrations of the base simulation and the sensitivity simulation, respectively, and ΔE denotes the percent change in Chinese emissions (we used 50% for ΔE in this study). When BFM is used, the contribution is sensitive to the emission perturbation rate [6,25,26]. Additionally, we chose 50% as the Chinese emission reduction since a reduction of 100% is unrealistic [27].

2.5. Receptor Definition

In this study, the analysis of the Chinese contribution was performed for two government tiers: 17 provinces and 250 prefectures in South Korea (Figure S1, supplementary materials). In this way, the receptor regions could be analyzed in detail for the different government tiers. For example, the 27-km simulation may be enough to analyze the source-receptor relationship over all of South Korea or the provincial boundaries. However, when we analyze the source-receptor relationship for the low government tier (prefectures) with the 27-km simulation, one modeling grid cell may contain multiple jurisdictions, as shown in Figure S2. Furthermore, South Korea has a complex coastline and a high population density in many areas. For these reasons, air quality simulations at a high resolution are needed when assessing the impact of foreign emissions on South Korea.

At the same time, air quality policy-making, implementation, and assessment are primarily conducted at air quality monitoring locations [28,29]. Usually, an air quality monitoring network is designed to reflect the monitoring purpose, e.g., exposure and large near-by emission sources. In South Korea, air quality monitors are often installed in downtown areas in proportion to population density and in the vicinity of industrial complexes where point source emissions are likely to be greater than in the other areas. Moreover, the relative contribution of foreign emissions may vary depending on the proximities of large emission sources to a specific receptor. To estimate the overall impacts of foreign and domestic emissions at the same time, we analyzed the foreign contribution in two ways: (1) modeling grid cells intersected by a receptor region (referred to as area-based hereafter; Figure S3a) and (2) choosing modeling grid cells where monitoring stations are located in a receptor region (referred to as monitor location-based hereafter; Figure S3b). During the latter approach, we excluded roadside monitoring stations when calculating foreign contributions to urban air pollution. The urban air quality monitoring network (AMS) was used to identify the location of the cells on the monitors in this study. Similar to previous studies [5–7,26,30], the area-based contributions are presented and discussed in Section 3.2–3.5. Moreover, we compare the foreign contributions with the two receptor definitions in Section 3.6.

3. Results and Discussion

3.1. Performance Evaluation of the WRF Simulation

We evaluated the performance of the meteorological simulation by comparing the values of the modeled meteorological variables with those of the measured variables (Figure 2). Meteorological variations throughout modeling periods affect the air quality modeling results (subsequently modeled contribution estimates), therefore we examined the Chinese contribution via long-term simulations to account for variable weather conditions over multiple years. For the purpose of evaluation, we calculated spatially averaged values at all METAR sites in China and South Korea for the 27-km simulation. The meteorology model performance evaluation is summarized in Table 3. Over the modeling period, the model underestimated the 2-m temperatures by 0.4 °C on average (the correlation coefficient (R) between the modeled and observed values was 1.0), and the normalized mean bias (NMB) was −4% to 1.3% and R was 0.95 to 0.99 for the seasonal analysis of the 2-m temperatures. Moreover, the model overestimated the 10-m wind speeds by 0.5 m/s on average (R = 0.8), which likely resulted in the faster transport of air pollutants in the model [13,31]. Especially, the 10-m wind speeds were overestimated in the winter by up to 0.8 m/s. We note that the overestimation of the wind speeds was most pronounced in coastal regions (Figure S4), which is consistent with the findings of Kim et al. [32].

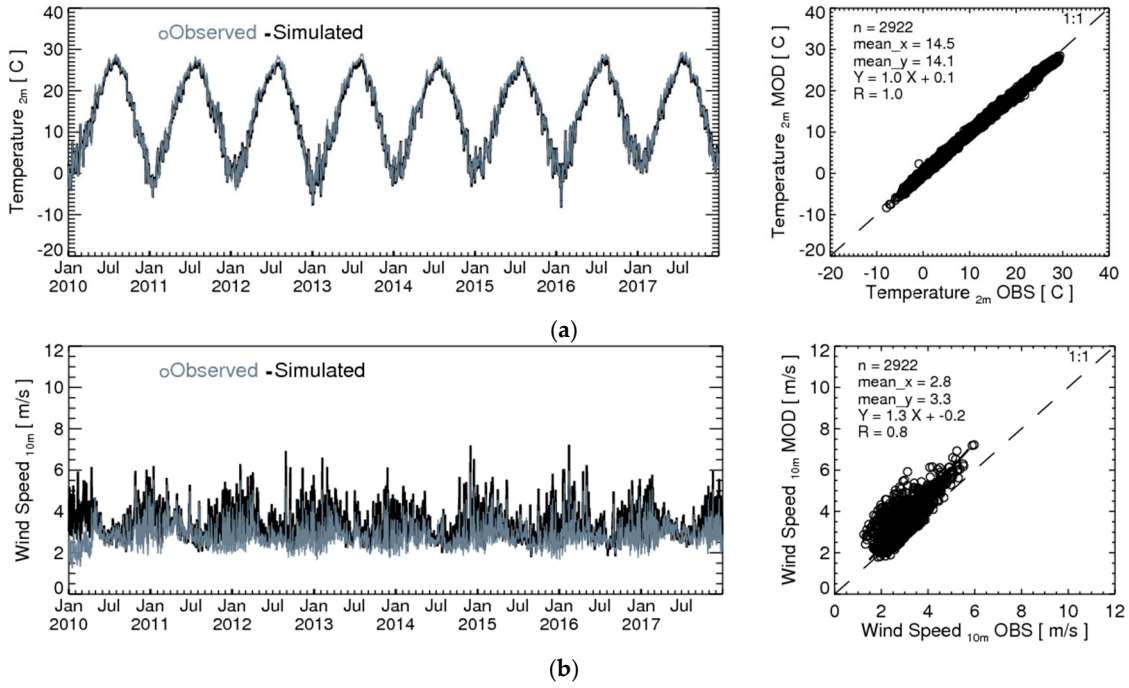

Figure 2. Comparisons of observed and simulated daily mean values of (**a**) 2-m temperatures and (**b**) 10-m wind speeds. These values were spatially averaged over 98 METeorological Aerodrome Reports (METAR) sites in South Korea and China.

Table 3. Comparison of the observed and simulated daily mean meteorological variables performance statistics across 98 METAR sites from 2010 to 2017 in South Korea and China.

Variable	Period	Observed Mean	Simulated Mean	Bias	NMB (%)	NME (%)	Correlation (R)	RMSE
2-m temperature (°C)	Period Mean	14.5	14.1	−0.4	−2.8	4.2	1.00	0.7
	Spring	13.8	13.3	−0.6	−4.0	5.7	0.99	1.0
	Summer	25.4	24.6	−0.8	−3.2	3.4	0.95	1.0
	Autumn	15.6	15.3	−0.4	−2.3	4.0	0.99	0.8
	Winter	1.7	1.8	0.1	1.3	27.5	0.99	0.7
10-m wind speed (m/s)	Period Mean	2.8	3.3	0.5	18.2	18.9	0.83	0.7
	Spring	3.0	3.4	0.4	14.8	17.1	0.78	0.7
	Summer	2.6	2.8	0.2	7.6	12.2	0.76	0.6
	Autumn	2.6	3.2	0.6	21.6	22.2	0.86	0.7
	Winter	2.8	3.6	0.8	27.9	28.7	0.86	0.9

3.2. Performance Evaluation of the Air Quality Modeling

For the performance evaluation of the $PM_{2.5}$ modeling, we compared the modeled and observed $PM_{2.5}$ concentrations after averaging the monthly mean $PM_{2.5}$ values across six supersites in South Korea (Figure 3). The annual simulated $PM_{2.5}$ concentration ranged from 17.4 to 20.5 μg/m^3, while the mean observed $PM_{2.5}$ concentration during the modeling period was 24.7 μg/m^3. Furthermore, the modeled $PM_{2.5}$ concentrations from the 27- and 9-km simulations were 18.5 and 20.0 μg/m^3, respectively. The underestimation of the $PM_{2.5}$ concentration can be attributed to multiple factors, such as overestimation of the wind speeds (see Section 3.1), uncertainty in the emissions inventory, and limitations of the CMAQ model. In general, the 9-km simulation was generally less biased and better correlated with the observations than the 27-km simulation across all of the supersites (Table 4). For the 9-km simulation, the R-value, NMB, normalized mean error (NME), and root-mean-squared error (RMSE) were 0.8, −19.2%, 20.3%, and 6.2 μg/m^3, respectively. Overall, we found little temporal variation in the model performance, except for in 2013 and 2014 for which the observed $PM_{2.5}$ concentrations were higher whereas the simulated concentrations were similar to those in other years. The difference between the observed and simulated values then gradually decreased over the following three years. As discussed in Section 3.1, the overestimation of the wind speeds in 2013 and 2014 likely led to the underestimation of the $PM_{2.5}$ concentration for 2013. When excluding 2013 and 2014, the NMBs of the 27- and 9-km simulations were −21% and −15%, respectively, which are in good agreement with the observations.

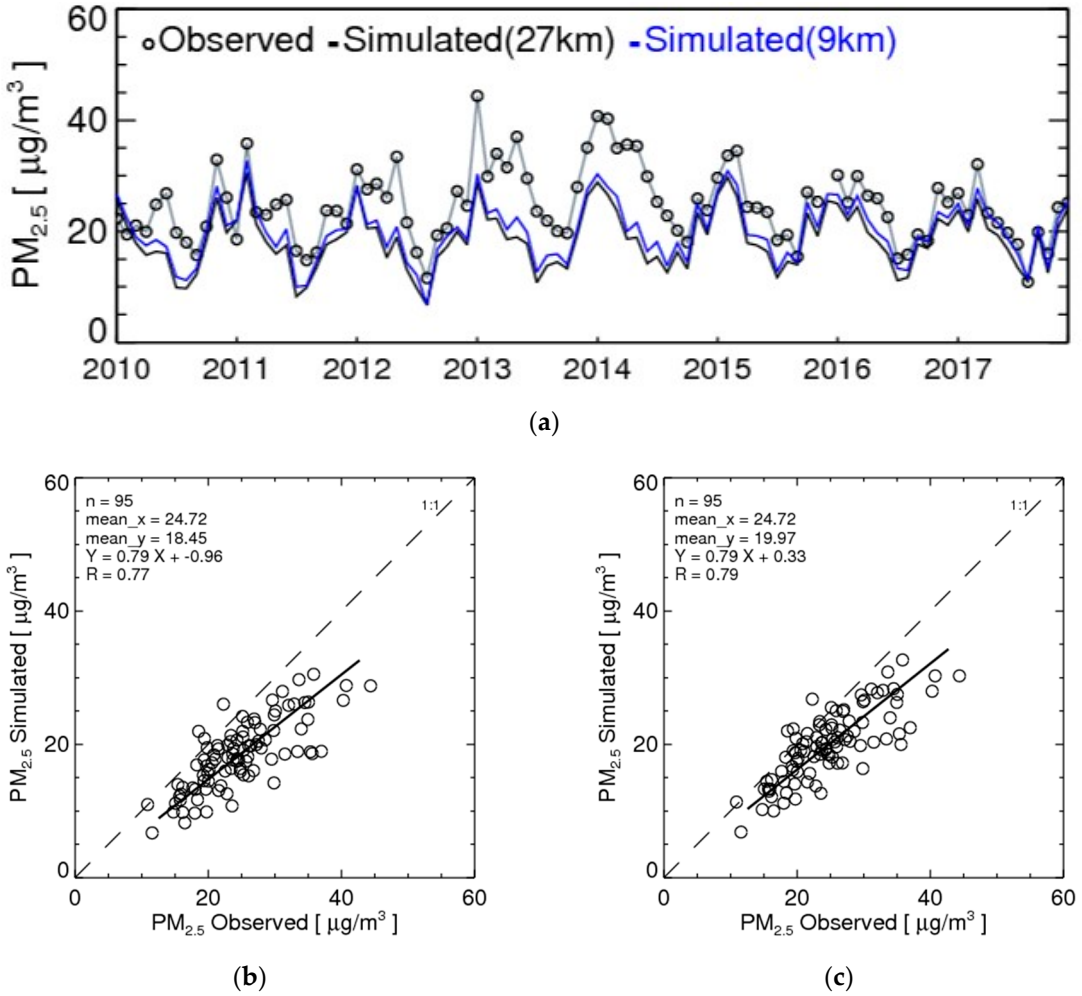

Figure 3. (**a**) Time series of the monthly means of the observed and the 27- and 9-km simulated particulate matter of 2.5 μm or less in diameter ($PM_{2.5}$) concentrations averaged across the six supersites in South Korea. Scatter plots of the (**b**) 27- and (**c**) 9-km simulations.

Table 4. Comparison of the monthly averages of the observed and simulated $PM_{2.5}$ concentrations and performance statistics for the 27- and 9-km simulations across the six supersites from 2010 to 2017.

Site	Simulation	Data Items	Observed Mean (μg/m³)	Simulated Mean (μg/m³)	Bias (μg/ m³)	NMB (%)	NME (%)	Correlation (R)	RMS μg/ m³)
Site average	27-km	95	24.7	18.5	−6.3	−25.4	26.1	0.77	7.6
	9-km			20.0	−4.8	−19.2	20.3	0.79	6.2
Baengnyeong	27-km	95	22.4	16.3	−6.2	−27.5	29.7	0.66	8.0
	9-km			16.2	−6.3	−27.9	30.1	0.64	8.2
Seoul Metropolitan Area	27-km	95	29.7	27.6	−2.2	−7.2	18.0	0.68	7.0
	9-km			28.2	−1.5	−5.2	15.8	0.76	6.2
Jungbu	27-km	83	30.4	20.9	−9.5	−31.2	34.5	0.69	12.4
	9-km			22.7	−7.7	−25.4	30.0	0.69	11.1
Honam	27-km	94	25.9	18.2	−7.7	−29.8	31.1	0.71	9.3
	9-km			20.6	−5.3	−20.5	23.0	0.74	7.2
Yeoungnam	27-km	57	22.6	19.3	-3.3	-14.5	19.5	0.63	5.7
	9-km			21.2	−1.3	−5.9	16.0	0.64	4.8
Jeju	27-km	69	15.9	9.8	−6.2	−38.7	39.3	0.68	7.6
	9-km			12.4	−3.5	−22.3	26.6	0.69	5.7

3.3. Spatial Distribution of the $PM_{2.5}$ Concentrations and Contributions

During the modeling period, the average $PM_{2.5}$ concentrations over South Korea with the 27- and 9-km simulations were 16 and 18 μg/m^3, respectively (Figure 4a,d). The $PM_{2.5}$ concentrations were high in SMA and in a part of Chungcheongnam-do (CCND, a western region in South Korea): ~21 μg/m^3 in both simulations. These are likely the results of high mobile emissions in SMA and large point sources for electric generation and petrochemical facilities in CCND [33]. We note that $PM_{2.5}$ concentrations around the West Sea, which is located close to China, were around 3 μg/m^3 higher than the East Sea.

Chinese ZOCs were high around the northwest region of South Korea (Figure 4b,e). In particular, the models reported greater than 10 μg/m^3 in the west part of South Korea and greater than 12 μg/m^3 in SMA. This is because pollutants emitted upwind are transported to South Korea and secondary $PM_{2.5}$ is formed through atmospheric chemical reactions with pollutants emitted from South Korea. Chinese ZOCs via the 9-km simulation were higher than those via the 27-km simulation. In particular, Gyeonggi and CCND showed Chinese ZOC differences of larger than 2 μg/m^3.

The average 27- and 9-km simulated Chinese contributions over South Korea were 58% and 56%, respectively. Overall, most regions in Korea including SMA showed a Chinese contribution of 45% or higher. Kim et al. [6] reported that the foreign contribution to the annual mean $PM_{2.5}$ concentration for SMA comprised over 60% in 2014. The Chinese contribution to the $PM_{2.5}$ concentration for SMA in February 2014 was 40–50% during high $PM_{2.5}$ days [32] and reached up to 70% at the Bulgwang supersite in Seoul [32]. The range in the Chinese contribution estimated in this study is similar to the results of the previous studies mentioned earlier [5,6,30]. The Chinese contribution was 70% or higher for the West Sea because of its geographic proximity to China and the primary wind direction in the winter and spring which makes bringing primary and secondary pollutants from China to South Korea favorable [34,35]. The Chinese contribution estimated via the 27-km simulation was higher than that via the 9-km simulation, especially in the West Sea, Jeju, and Gangwon. The West Sea comprises many islands that are part of Incheon, Jeollanam-do (JLND), and Jeollabuk-do (JLBD), and this geographic feature could have led to the differences between the two simulations in the local contribution analysis.

We note that the Chinese contribution was equal to or less than 40% in regions where $PM_{2.5}$ concentrations were over 25 μg/m^3 (SMA and a part of CCND) and the Chinese ZOCs were relatively high. This is probably because the Chinese contribution was determined as relatively small in regions with large local emissions such as mobile sources and large point sources. Conversely, the Chinese contribution is estimated to be relatively high in regions with small local emissions and low annual mean $PM_{2.5}$ concentrations. This is likely to be because the low local emissions have little impact on the local $PM_{2.5}$ concentration compared to the contribution of the Chinese emissions. Spatial gradients in simulated concentration fields are relatively gentle in SMA, CCND, and Chungcheongbuk-do (CCBD) but relatively steep in Gangwon and JLND, possibly due to the mountains in the center of those provinces.

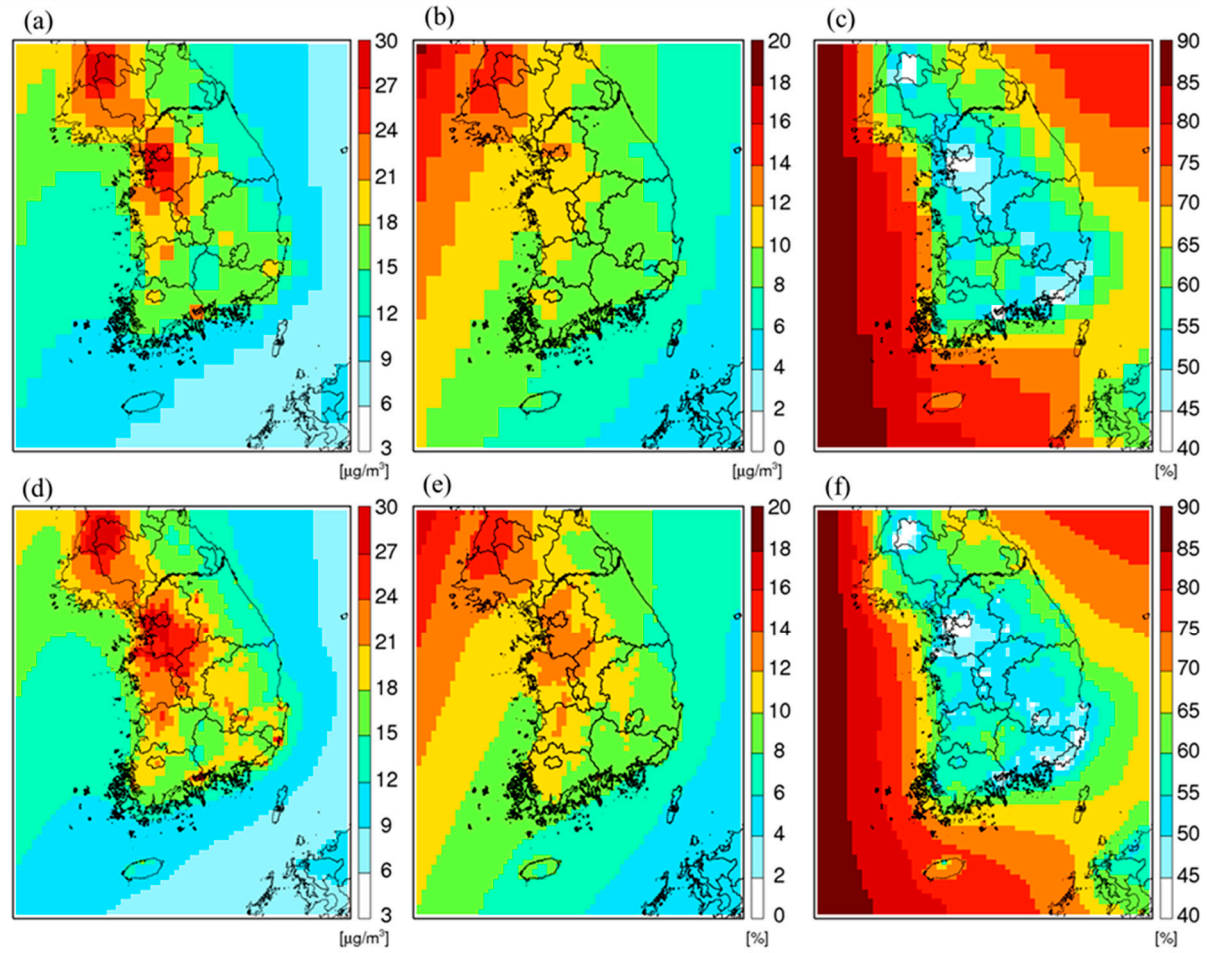

Figure 4. (**a**,**d**) Period mean $PM_{2.5}$ concentrations, (**b**,**e**) Chinese zero-out contribution (ZOCs), and (**c**,**f**) the Chinese contribution in the 27- (**a**–**c**) and 9-km (**d**–**f**) simulations from 2010 to 2017.

3.4. The Chinese Contribution to the $PM_{2.5}$ Concentrations in the Two Government Tiers

Figure 5 shows a comparison of the 27-km and 9-km simulated Chinese contributions to $PM_{2.5}$ in the individual jurisdictional areas. For the 17 provinces, the mean the 27- and 9-km simulated Chinese contributions were 54.2% and 52.9%, respectively, while for the 250 prefectures, they were 52.4% and 50.8%, respectively. The overall means of the relative Chinese contributions between the two model simulations differed by less than 5% regardless of the government boundary tier used in the average contribution calculations. However, we noticed that the range in the estimated Chinese contribution in individual jurisdictions was quite wide. The 27- and 9-km simulations showed little difference in our contribution analysis for the 17 provinces (Figure 5b). For the 250 prefectures, the contribution differences via the two simulations were consistent in many areas but at the same time, we also observed that many prefectures with less than 50% Chinese contribution showed estimated contribution differences of up to 10% due to the modeling grid resolution (Figure 5c). The size of the difference was large enough to change the primary contributor for these areas, thus it may be crucial to consider this when developing air quality improvement policies. In addition, the difference between the Chinese contribution estimated via the two simulations was particularly large in coastal areas (GSND, Gangwon, and JLND). In a relative sense, decreasing the Chinese contribution means increasing the domestic contribution, thus considering the modeling grid resolutions seems to be critical for the quantitative assessment of the foreign contribution. That is to say, the contribution from domestic emissions is likely to be underestimated if we use a coarse-grid resolution.

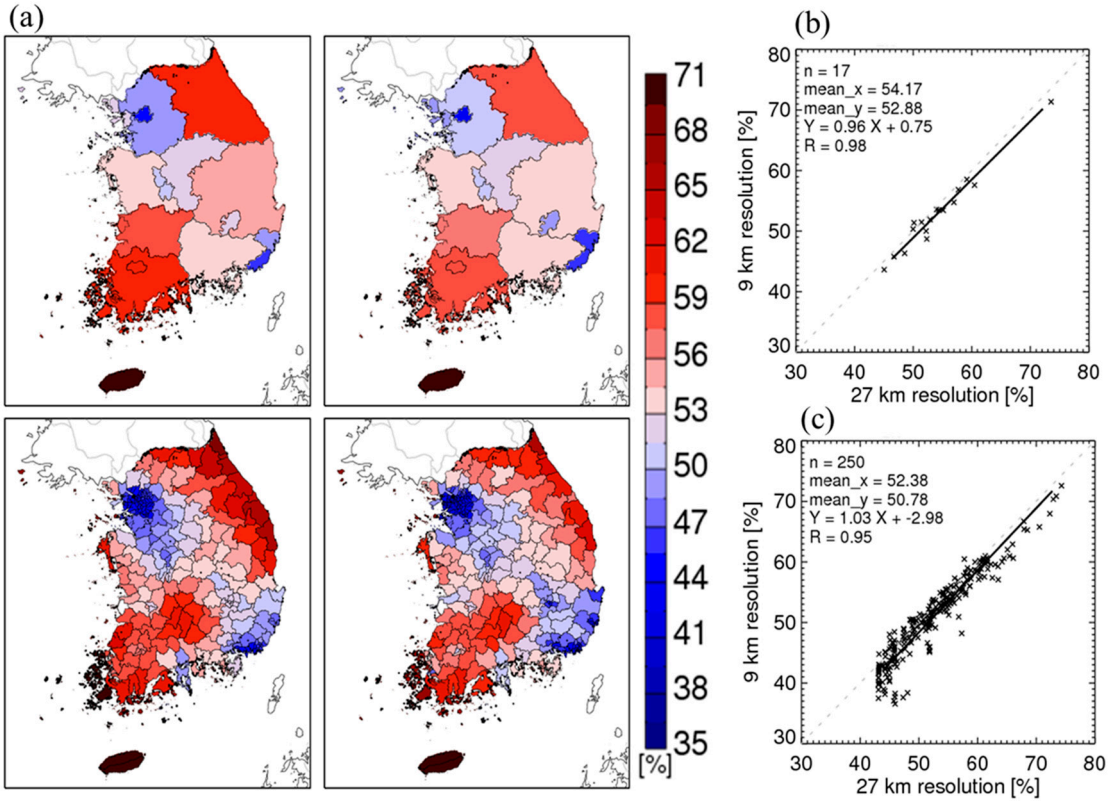

Figure 5. The eight-year mean Chinese contribution to $PM_{2.5}$ concentrations in 17 provinces (**a-top**) and 250 prefectures (**a-bottom**) in South Korea estimated via the 27- (**a-left**) and 9-km (**a-right**) simulations from 2010 to 2017. Scatter plots of the Chinese contribution estimated via the 27- and 9-km simulations for (**b**) the 17 provinces and (**c**) the 250 prefectures.

3.5. Monthly Variation in the Chinese Contribution

In general, the monthly mean observed and simulated $PM_{2.5}$ concentrations were high in the cold season (January–March) and low in the summer months (July and August) (Figure 6). In detail, the Chinese contribution was more than 60% for November–March and less than 40% for August–September. The monthly variation in the Chinese contribution is consistent with the $PM_{2.5}$ monthly variations (Figure 3a), which is likely caused by the frequent inflow of air sheds from China in the spring and winter via northwesterly winds [36]. Conversely, as the winds become weaker in the summer and autumn, domestic emissions make a greater contribution. The influence of Chinese emissions is also less during the summer months than winter months because of more frequent rainfall and stronger easterly and southerly winds [37]. The difference between the 10th and 90th percentiles of the monthly Chinese contribution in individual jurisdictions was approximately 20% on average. This means that the Chinese contribution varied considerably among South Korean regions depending on location.

The discrepancies in the spatially averaged monthly Chinese contribution between the 27- and 9-km simulations were consistent except in July–September when low $PM_{2.5}$ concentrations and the Chinese contribution were estimated. In general, the monthly Chinese contribution via the 27-km simulation was 5–10% higher than via the 9-km simulation. These results suggest that the Chinese contribution estimated via the two simulations can vary not only in space but also in time. In summary, when air quality improvement plans are developed based on simulations with a higher grid resolution (i.e., 9 km), more detail of the source-receptor relationship at a local level should be examined. For this reason, we analyzed the results of the 9-km simulation, as reported in the following sections.

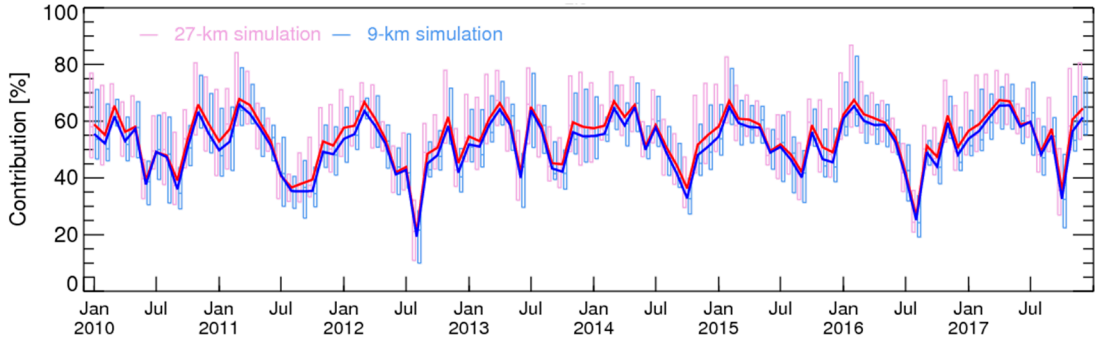

Figure 6. The monthly Chinese contribution to the $PM_{2.5}$ concentrations of 17 provinces. The solid lines depict the average Chinese contribution.

3.6. Dependency of the Chinese Contribution on Receptor Definition

In this section, we compared the Chinese emission contributions to the South Korean $PM_{2.5}$ concentrations with two receptor definitions: (1) area-based and (2) monitor location-based utilizing the 9-km simulation. The monitor location-based Chinese contribution accounted for approximately 45% of the 8-year average $PM_{2.5}$ concentrations (Figure 7). Differences in the Chinese contribution between the two receptor definitions were not significant for densely populated cities such as Seoul, Daejeon, Sejong, and Gwangju. This is because of the relatively small sizes of the cities (except for Seoul) and the fact that all of the grids in Seoul are equipped with monitor stations. In contrast, the difference in the Chinese contribution via the two receptor definitions was greater for Incheon, JLND, JLBD, and Jeju with a range of 10–15%. The large difference for Incheon is likely due to the inclusion of the islands in the West Sea that have a high Chinese contribution in the relatively low $PM_{2.5}$ concentrations, the geographical proximity to China, and the low domestic emissions with modeling grid cells encompassed by the jurisdictional boundary. The large variations for JLND, JLBD, and Gangwon were probably caused by the uneven distribution of the monitoring stations in these regions, as well as the steep horizontal gradients of $PM_{2.5}$ concentration and the Chinese contribution. Figure S5 shows a similar result with the 27-km simulation for the receptor definition.

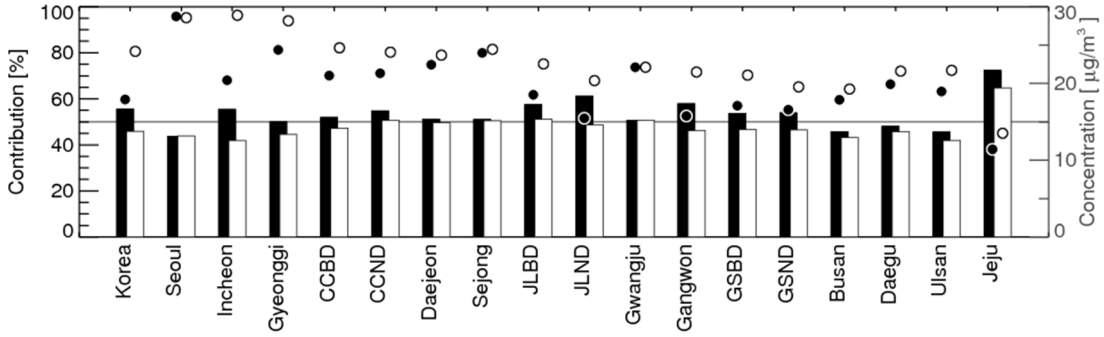

Figure 7. The eight-year average $PM_{2.5}$ concentrations (circles) and the Chinese contribution (bars) in the 17 provinces via the 9-km simulation. The black and white colors represent the area-based and monitor location-based Chinese contribution, respectively.

The monitor location-based Chinese contribution to $PM_{2.5}$ concentrations in the summer and autumn ranged from 30–45% for most provinces except for Jeju where the Chinese contribution reached 60% (Figure 8). The underestimation of the local emission in Jeju might have caused the high Chinese ZOCs. For the spring and winter, the monitor location-based Chinese contribution was 15% higher than in the summer and autumn. Moreover, the monitor location-based Chinese contribution was generally 10% lower than the area-based Chinese contribution. The same analysis conducted with the 27-km simulation exhibited approximately 5% higher Chinese contributions than those via the 9-km simulation (Figure S6). The interannual variability of seasonal Chinese contributions increased largely in the summer months. This is probably because of local and synoptic

meteorological events such as the rainy season, local rainfall, typhoons, and the El Niño–Southern Oscillation (ENSO) [38–40].

Both the 27- and 9-km simulations showed similar spatial variability across all of the regions. In South Korea, monitoring stations are set up based on the population size, so they are mostly in areas with higher domestic emissions (such as downtown areas). The difference in the Chinese contribution estimated using the two receptor definitions was the largest (approximately 20%) for the Gangwon region. Even though Gangwon has large areas, it has monitoring stations in only a handful of cities (Wonju, Chuncheon, Gangneung, and Donghae). In summary, estimates of domestic and foreign contributions can be affected by the distribution of the monitoring stations and local emissions which depend on population, industry, and traffic. The annual variation of Chinese contributions at the 9-km simulation is 46% $\pm$ 2.3% (monitor location-based), and the differences between the two grid resolutions and the two receptor definitions were around 5% and 10%, respectively (Figure S7).

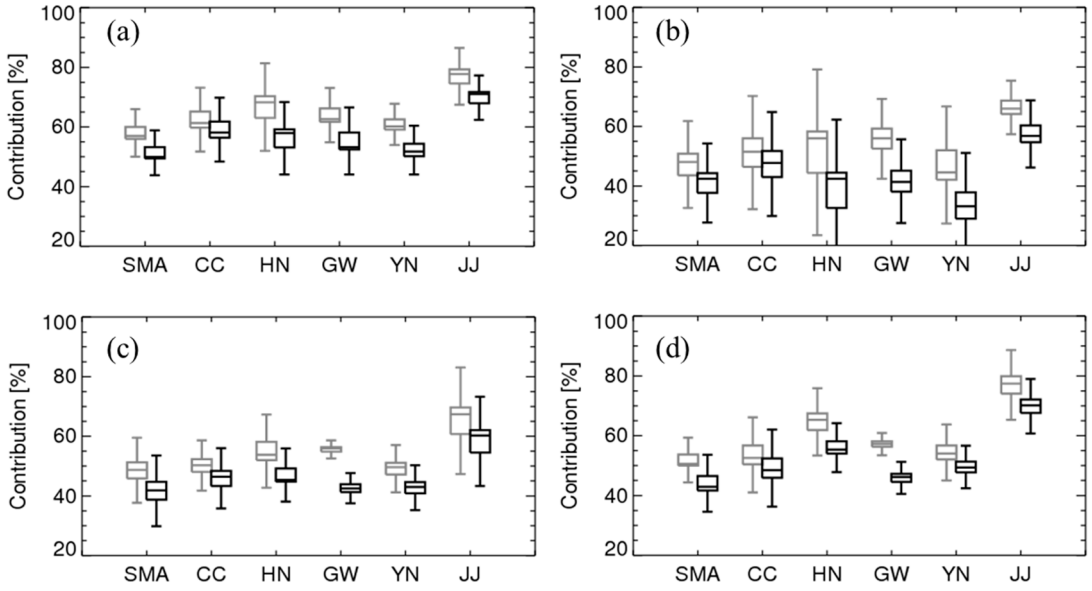

Figure 8. Variations in the Chinese contribution to seasonal mean $PM_{2.5}$ concentrations in the high-tier government boundaries in South Korea from 2010 to 2017 estimated via the 9-km simulation: (**a**) spring (March–May), (**b**) summer (June–August), (**c**) autumn (September–November), and (**d**) winter (December–February). The gray and black boxes represent the area-based and the monitor location-based Chinese contribution, respectively.

4. Conclusions

In this study, we examined source-receptor relationships for $PM_{2.5}$ concentrations in South Korea for the period of 2010–2017. In particular, we analyzed variabilities in the relative Chinese contribution to $PM_{2.5}$ concentrations in South Korea by modeling grid resolutions (27- and 9-km), meteorological variability (monthly, seasonal, and interannual), and definitions of receptors. For this study, the Chinese contribution to the $PM_{2.5}$ concentration in South Korea was estimated as ZOC with two nested grid simulations with/without a 50% Chinese emission perturbation in the coarse-grid domain.

We observed that the difference in the Chinese contribution between the 27- and 9-km simulations was greater when the receptor areas were smaller: 4% in the 17 provinces and 10% in the 250 prefectures on average. We note that local emission impacts and the clear distinction between the land and the ocean in the high-resolution simulation could have contributed to these contribution differences. Furthermore, we found that this pattern was more obvious in the spring and winter seasons when the Chinese contribution was the highest. Last, we found that the estimated Chinese contribution was approximately 10% higher when the receptors were defined as whole grid cells

within jurisdictional boundaries compared with receptors composed of grid cells at monitoring stations. The difference was likely caused by the population-based placement of air quality monitoring stations, thus Seoul, where a dense network of monitoring stations is available, shows little differences in the estimated Chinese contribution regardless of receptor definition. However, for regions with an uneven distribution of monitors (such as Incheon, JLND, JLBD, and Gangwon), we observed that differences in the Chinese contribution were 10%–15% due to the difference in the receptor definitions.

In summary, we found that the relative Chinese contribution varied by modeling grid resolution and how receptors were defined. The 9-km simulation can better represent coastal lines and jurisdictional boundaries (especially the prefectures), therefore we believe that fine-grid modeling can estimate the effects of local emissions better than coarse-grid modeling. Therefore, it is advisable to use high-resolution modeling results for regional contribution analysis when developing air quality action plans. In addition, we recommend considering how receptors should be defined depending on the purpose of contribution analysis and the application of the analysis results. If population exposure needs to be addressed, it is desirable to use modeling grid cells at monitor locations.

For more practical applications, we recommend using the most up-to-date emission data in the future because Chinese emissions have been rapidly decreasing recently. In addition, future research will need to include an investigation on the Chinese contribution to $PM_{2.5}$ components such as nitrate and sulfate in South Korea. Last, although we focused on source-receptor relationships in Northeast Asia, we believe that the analysis approach we have developed is also applicable to any region where modeling grid resolutions and jurisdictional boundaries need to be considered for a contribution assessment.

Supplementary Materials: The following are available online at www.mdpi.com/link, Figure S1: The two government tiers in South Korea: (**a**) 17 provinces with an area of 5874 km^2 on average and (**b**) 250 prefectures with an area of 382 km^2 on average, Figure S2: Spatial scale comparison of the 27-km modeling grid cells and jurisdictional boundaries. The black and gray lines represent the boundaries of the provincial and prefectural areas, respectively, Figure S3: An illustration of the receptor definitions used in the study: (**a**) modeling grid cells intersected by a receptor region ('area-based'), and (**b**) choosing modeling grid cells where monitoring stations (red dots) are located in a receptor region ('monitor location-based') in Gyeonggi province, Figure S4: The Spatial distributions of the observed and estimated via the 27-km simulation with 10-m wind and the difference during 2010–2017, Figure S5: The eight-year average $PM_{2.5}$ concentration (circles) and Chinese contribution (bars) in 17 provincial areas via the 27-km simulation. The black and white colors represent the area-based and monitor location-based Chinese contribution, respectively, Figure S6: Variations in the Chinese contribution in the high-tier government boundaries estimated via the 27-km simulation to seasonal mean $PM_{2.5}$ concentrations over South Korea from 2010 to 2017: (**a**) spring (March–May), (**b**) summer (June–August), (**c**) autumn (September–November), and (**d**) winter (December–February). The Gray and black boxes represent the area-based and monitor location-based Chinese contribution, respectively, Figure S7: The annual variability at the simulations of the 27- (solid line) and 9-km (dotted line) simulations during 2010 to 2017 over South Korea. The pink and blue colors represent the area-based and monitor location-based Chinese contribution, respectively.

Author Contributions: All authors have read and agree to the published version of the manuscript. Conceptualization, M.B. and S.K.; methodology, M.B. and S.K.; project administration, S.K.; visualization, M.B.; writing—original draft, M.B.; writing—review and editing, M.B., B.-U.K., H.C.K., and S.K. All authors have read and agreed to the published version of the manuscript.

Funding: The study was supported by the National Strategic Project-Fine Particle of the National Research Foundation of Korea (NRF) and funded by the Ministry of Science and ICT (MSIT), the Ministry of Environment (ME), and the Ministry of Health and Welfare (MOHW) (2017M3D8A1092015) in South Korea.

Conflicts of Interest: The scientific results and conclusions, as well as any views or opinions expressed herein, are those of the author(s) and do not necessarily reflect the views of NOAA or the Department of Commerce.

References

1. *Annual Report of Air Quality in Korea 2018*; National Institute of Environmental Research: Incheon, Korea, 2019 .
2. Yoo, C.; Lee, D.-G.; Lee, Y.-M.; Lee, M.-H.; Hong, J.-H.; Lee, S.-J. Methodology of Application to Air Quality Model to Evaluate the Results of the Enforcement Plan in Seoul Metropolitan Area. *JESI* **2011**, *20*, 1647–1661.
3. Kim, E.; Bae, C.; Yoo, C.; Kim, B.-U.; Kim, H.C.; Kim, S. Evaluation of the Effectiveness of Emission Control Measures to Improve PM2.5 Concentration in South Korea. *J. Korean Soc. Atmos. Environ.* **2018**, *34*, 469–485.
4. Guidance on the Use of Models and Other Analyses for Demonstrating Attainment of Air Quality Goals for Ozone, PM2.5 and Regional Haze; U.S. Environmental Protection Agency: Washington, DC, USA, 2007.
5. Choi, J.; Park, R.J.; Lee, H.-M.; Lee, S.; Jo, D.S.; Jeong, J.I.; Henze, D.K.; Woo, J.-H.; Ban, S.-J.; Lee, M.-D.; et al. Impacts of local vs. Trans-boundary emissions from different sectors on PM2.5 exposure in South Korea during the KORUS-AQ campaign. *Atmos. Environ.* **2019**, *203*, 196–205.
6. Kim, H.C.; Kim, E.; Bae, C.; Cho, J.H.; Kim, B.-U.; Kim, S. Regional contributions to particulate matter concentration in the Seoul metropolitan area, South Korea: seasonal variation and sensitivity to meteorology and emissions inventory. *Atmos. Chem. Phys.* **2017**, *17*, 10315–10332.
7. Uno, I.; Osada, K.; Yumimoto, K.; Wang, Z.; Itahashi, S.; Pan, X.; Hara, Y.; Yamamoto, S.; Nishizawa, T. Importance of Long-Range Nitrate Transport Based on Long-Term Observation and Modeling of Dust and Pollutants over East Asia. *Aerosol Air Qual. Res.* **2017**, *17*, 3052–3064.
8. Itahashi, S.; Uno, I.; Kim, S. Source Contributions of Sulfate Aerosol over East Asia Estimated by CMAQ-DDM. *Environ. Sci. Technol.* **2012**, *46*, 6733–6741.
9. Han, C.; Kim, S.; Lim, Y.-H.; Bae, H.-J.; Hong, Y.-C. Spatial and Temporal Trends of Number of Deaths Attributable to Ambient PM2.5 in the Korea. *J. Korean Med. Sci.* **2018**, *33*, 193.
10. Lee, J.-H.; Lee, S.-H.; Kim, H.C. Detection of Strong NOX Emissions from Fine-scale Reconstruction of the OMI Tropospheric NO2 Product. *Remote Sens* **2019**, *11*, 1861.
11. Cohan, D.S.; Hu, Y.; Russell, A.G. Dependence of ozone sensitivity analysis on grid resolution. *Atmos. Environ.* **2006**, *40*, 126–135.
12. Jiang, X.; Yoo, E. The importance of spatial resolutions of Community Multiscale Air Quality (CMAQ) models on health impact assessment. *Sci. Total Environ.* **2018**, *627*, 1528–1543.
13. Kim, H.C.; Kim, S.; Kim, B.-U.; Jin, C.-S.; Hong, S.; Park, R.; Son, S.-W.; Bae, C.; Bae, M.; Song, C.-K.; et al. Recent increase of surface particulate matter concentrations in the Seoul Metropolitan Area, Korea. *Sci. Rep.* **2017**, *7*, 4710.
14. Pei, L.; Yan, Z.; Sun, Z.; Miao, S.; Yao, Y. Increasing persistent haze in Beijing: potential impacts of weakening East Asian winter monsoons associated with northwestern Pacific sea surface temperature trends. *Atmos. Chem. Phys.* **2018**, *18*, 3173–3183.
15. Byun, D.; Schere, K.L. Review of the Governing Equations, Computational Algorithms, and Other Components of the Models-3 Community Multiscale Air Quality (CMAQ) Modeling System. *Appl. Mech. Rev.* **2006**, *59*, 51–77.
16. Skamarock, W.; Klemp, J.; Dudhia, J.; Gill, D.; Barker, M.; Duda, K.; Huang, -Y; Wang, W.; Powers, J. *A description of the Advanced Research WRF Version 3*; 2008; pp. 1–113;.
17. Guenther, C.C. Estimates of global terrestrial isoprene emissions using MEGAN (Model of Emissions of Gases and Aerosols from Nature). *Atmos. Chem. Phys.* **2006**, *6*, 3181–3210.
18. Benjey, W.; Houyoux, M.; Susick, J. Implementation of the SMOKE emission data processor and smoke tool input data processor in models-3. In Proceedings of the Emission Inventory Conference, Denver, CO, USA, 1–4 May 2001.
19. *NCEP FNL Operational Model Global Tropospheric Analyses, continuing from July 1999*; Research Data Archive at the National Center for Atmospheric Research, Computational and Information Systems Laboratory: Boulder CO, USA, 2000.
20. Lee, D.; Lee, Y.-M.; Jang, K.-W.; Yoo, C.; Kang, K.-H.; Lee, J.-H.; Jung, S.-W.; Park, J.-M.; Lee, S.-B.; Han, J.-S.; et al. Korean National Emissions Inventory System and 2007 Air Pollutant Emissions. *Asian J. Atmos. Environ.* **2011**, *5*, 278–291.
21. Li, M.; Zhang, Q.; Kurokawa, J.; Woo, J.-H.; He, K.; Lu, Z.; Ohara, T.; Song, Y.; Streets, D.G.; Carmichael, G.R.; et al. MIX: A Mosaic Asian Anthropogenic emissioni nventory Under The International Collaboration Framework of The MICS-Asia and HTAP. *Atmos. Chem. Phys.* **2017**, *17*, 935–963.

22. Carter, W.P.L. *Implementation of the SAPRC-99 Chemical Mechanism into the Models-3 Framework*; Report to the United States Environmental Protection Agency; United States Environmental Protection Agency: Washington, DC, USA, 2000; p. 29
23. Tan, J.; Zhang, Y.; Ma, W.; Yu, Q.; Wang, J.; Chen, L. Impact of spatial resolution on air quality simulation: A case study in a highly industrialized area in Shanghai, China. *Atmos. Pollut. Res.* **2015**, *6*, 322–333.
24. Fountoukis, C.; Koraj, Dh.; Denier van der Gon, H.A.C.; Charalampidis, P.E.; Pilinis, C.; Pandis, S.N. Impact of grid resolution on the predicted fine PM by a regional 3-D chemical transport model. *Atmos. Environ.* **2013**, *68*, 24–32.
25. Kim, S.; Bae, C.; Yoo, C.; Kim, B.-U.; Kim, H.C.; Moon, N. PM2.5 Simulations for the Seoul Metropolitan Area: (II) Estimation of Self-Contributions and Emission-to-PM2.5 Conversion Rates for Each Source Category. *J. Korean Soc. Atmos. Environ.* **2017**, *33*, 377–392.
26. Koo, B.; Wilson, G.M.; Morris, R.E.; Dunker, A.M.; Yarwood, G. Comparison of Source Apportionment and Sensitivity Analysis in a Particulate Matter Air Quality Model. *Environ. Sci. Technol.* **2009**, *43*, 6669–6675.
27. Bartnicki, J. Computing Source-Receptor Matrices with the EMEP Eulerian Acid Deposition Model; Norwegian Met. Inst.: Oslo, Norway, 1999.
28. Modeling Guidance for Demonstrating Air Quality Goals for Ozone, PM2.5, and Regional Haze. U.S. Environmental Protection Agency: Washington, DC, USA, 2018.
29. Emery, C.; Liu, Z.; Russell, A.G.; Odman, M.T.; Yarwood, G.; Kumar, N. Recommendations on statistics and benchmarks to assess photochemical model performance. *J. Air Waste Manag. Assoc.* **2017**, *67*, 582–598.
30. Bae, C.; Kim, B.-U.; Kim, H.C.; Yoo, C.; Kim, S. Long-Range Transport Influence on Key Chemical Components of PM2.5 in the Seoul Metropolitan Area, South Korea, during the Years 2012–2016. *Atmosphere* **2020**, *11*, 48.
31. Hawkins, T.W.; Holland, L.A. Synoptic and Local Weather Conditions Associated with PM2.5 Concentration in Carlisle, Pennsylvania. *Middle States Geographer.* **2010**, *43*, 72–84.
32. Kim, J.-H.; Choi, D.-R.; Koo, Y.-S.; Lee, J.-B.; Park, H.-J. Analysis of Domestic and Foreign Contributions using DDM in CMAQ during Particulate Matter Episode Period of February 2014 in Seoul. *J. Korean Soc. Atmos. Environ.* **2016**, *32*, 82–99.
33. Kim, S.; Kim, O.; Kim, B.-U.; Kim, H.C. Impact of Emissions from Major Point Sources in Chungcheongnam-do on Surface Fine Particulate Matter Concentration in the Surrounding Area. *J. Korean Soc. Atmos. Environ.* **2017**, *33*, 159–173.
34. Itahashi, S.; Uno, I.; Osada, K.; Kamiguchi, Y.; Yamamoto, S.; Tamura, K.; Wang, Z.; Kurosaki, Y.; Kanaya, Y. Nitrate transboundary heavy pollution over East Asia in winter. *Atmos. Chem. Phys.* **2017**, *17*, 3823–3843.
35. Kim, B.-U.; Bae, C.; Kim, H.C.; Kim, E.; Kim, S. Spatially and chemically resolved source apportionment analysis: Case study of high particulate matter event. *Atmos. Environ.* **2017**, *162*, 55–70.
36. Liu, H. Transport pathways for Asian pollution outflow over the Pacific: Interannual and seasonal variations. *J. Geophys. Res.* **2003**, *108*, 8786.
37. Baek, S.; Kim, H.; Chang, H. Optimal Hybrid Renewable Power System for an Emerging Island of South Korea: The Case of Yeongjong Island. *Sustainability* **2015**, *7*, 13985–14001.
38. Ho, C.-H.; Baik, J.-J.; Kim, J.-H.; Gong, D.-Y.; Sui, C.-H. Interdecadal Changes in Summertime Typhoon Tracks. *J. Clim.* **2004**, *17*, 10.
39. Zhang, L.; Liao, H.; Li, J. Impacts of Asian summer monsoon on seasonal and interannual variations of aerosols over eastern China. *J. Geophys. Res. Atmos.* **2010**, *115*.
40. Lee, J.H.; Julien, P.Y. ENSO impacts on temperature over South Korea: ENSO impacts on temperature over South Korea. *Int. J. Climatol.* **2016**, *36*, 3651–3663.